

Fig. 2. The pyroxene quadrilateral. Circles, electron-probe analysis from a single grain; triangles, unmixed pairs of pyroxenes determined by single-crystal x-ray diffraction; squares, estimated bulk composition of pairs.

tion gave a glass with a refractive index 1.550 (± 0.001) corresponding to An_{74} (5). Electron-probe analyses suggested a range from An_{72} to An_{89} within single grains.

The ilmenite in this rock is relatively free of shock lamellae and has a low density of dislocations and stacking faults. Twinning lamellae are rare, and there is no sign of compositional zoning or inhomogeneities within grains. The $TiO_2:FeO$ ratio is 60:40, but small variations from grain to grain are observed. X-ray powder diffraction from an ilmenite separate gave cell parameters $a_{hex} = 5.08$, $c_{hex} = 14.06 \pm 0.01$ Å.

Troilite is the second most abundant opaque phase (~0.1 percent). It usually contains minute blebs of native iron. Electron-probe analyses show the blebs to be virtually free of Ni and Co, in contrast to the iron spherules in the glassy breccia and to meteoritic iron.

Minor amounts of ulvöspinel (<0.01 percent) occur in association with ilmenite and native iron. Textural evidence suggests that spinel may have formed after ilmenite (a postcrystallization "thermal event"). This possibility is further supported by the occasional occurrence of troilite on minute cracks and fissures.

A small amount of apatite in hexagonal prisms has been seen optically, and its presence has been confirmed by microprobe. Cristobalite (mean r. i. 1.487) with characteristic twinning and tile structure occurs in euhedral crystals and filling interstices, and the presence of acicular tridymite (mean r. i. 1.472) in parallel growth with pyroxene was confirmed by x-ray single-crystal diffraction. A few crystals of K-feldspar were identified optically and by microprobe.

The yellow mineral referred to in the Preliminary Examination Team report (6) has been observed, and its cell

parameters are being determined. A small amount of purplish mineral with hexagonal habit and a dark brown mineral have also been seen, but the minerals have not been identified.

X-ray fluorescence analysis of 0.5 g of rock 10044 gave the following concentrations: Nb, 41 ppm; Zr, 465 ppm; Y, 215 ppm; Sr, 250 ppm; and Cr, 1180 ppm. Semiquantitative analyses showed that the chromium is present in approximately equal amounts in the light pyroxene fraction and the ore fraction, with lesser amounts in the dense pyroxene fraction.

We also made trace element determinations on 0.5-g samples of rocks 10045 and 10060, which gave Nb, 28 and 38 ppm; Zr, 300 and 565 ppm; Y, 190 and 170 ppm; Sr, 185 and 225 ppm; and Cr 3010 and 2165 ppm.

The lobate embayed textures of the ilmenites and the arrangement of the plagioclase and pyroxene within the lobes suggest that ilmenite was the first phase to begin to crystallize. It was probably soon followed by pyroxene, which shows clear centers to the crystals but plagioclase enclosed in the outer parts. Tridymite is involved in intergrowths with pyroxene and plagioclase and in at least one case with K-feldspar, so it probably crystallized fairly late.

Mineralogy and Deformation in Some Lunar Samples

Abstract. *Observations on the mineralogy and deformation in samples of crystalline rocks, breccias, and fines from Tranquillity Base provide evidence for magmatic and impact processes. Overall homogeneity, igneous textures, and absence of xenoliths in the crystalline rocks indicate derivation from a common titanium-rich magma by internal, anorogenic volcanism rather than by impact. Crystallization conditions allowed strong compositional variation in pyroxenes, olivine, and plagioclase and the growth of a new mineral, the iron analog of pyroxmangite. Subsequently, impact produced breccias containing shock-deformed crystals and glasses of varying compositions.*

The preliminary examination (1) has shown that the Tranquillity Base rocks have undergone igneous and deformational processes in many ways comparable with terrestrial and meteoritic phenomena. The major minerals can be assigned to known rock-forming mineral groups, but their compositional variation, association, and textures demonstrate relationships which complement and extend petrological experience gained from investigations of terrestrial basic rocks and meteorites and from synthetic studies. To this end we have examined four crystalline rocks,

The compositions and mutual relation of the opaque minerals can be used to put limits on fS_2 and fO_2 .

For the general evolution of moon rocks we would conjecture that, since lunar gravity and thermal gradient are both low, there has been no crust-mantle recycling. Low-melting silicates may have formed an original crust later to be partially covered by the basic rocks now reported. These may have originated in a deep magma chamber floored by phases in the system Ni-Fe-S.

J. C. BAILEY, P. E. CHAMPNESS

A. C. DUNHAM, J. ESSON

W. S. FYFE, W. S. MACKENZIE

E. F. STUMPFL, J. ZUSSMAN

Department of Geology,

The University,

Manchester M13 9 PL, England

References and Notes

1. A. El Goresy, in *Shock Metamorphism of Natural Materials*, B. M. French and N. M. Short, Eds. (Mono, Baltimore, 1968), pp. 531-53.
 2. M. G. Brown and P. Gay, *Am. Mineral.* **44**, 592-602 (1959).
 3. G. M. Brown, *ibid.*, **45**, 15-38 (1960).
 4. K. Viswanathan, *ibid.* **51**, 429-42 (1966).
 5. J. R. Smith, *Carnegie Inst. Wash. Yearbook* No. 56 (1957), p. 216.
 6. Lunar Sample Preliminary Examination Team, *Science* **165**, 1211 (1969).
 7. We thank the Department of Mineralogy and Petrology, University of Cambridge, for mineral separates and loan of a spindle stage, D. L. Hamilton for melting the plagioclases, and J. E. Chisholm for help with x-ray work.
- 4 January 1970

compositional variation reflect incomplete equilibration between minerals and liquid during crystallization.

Clinopyroxene shows extreme variation in composition (Fig. 1A), with single grains having domains of varying Ca/Mg and Mg/Fe ratios. The majority of the compositions plot in a band across the pyroxene quadrilateral from approximately $\text{Ca}_{40}\text{Mg}_{43}\text{Fe}_{17}$ to $\text{Ca}_{25}\text{Mg}_5\text{Fe}_{70}$. Large parts of this trend are commonly present within systematically zoned grains, and Fig. 1B shows the variation along a traverse of 0.8 mm.

The unidentified yellow mineral (I) has been studied in detail in 10047. It occurs as discrete grains associated with cristobalite and as marginal growths on clinopyroxene. Unlike the clinopyroxene, it is homogeneous; the composition, averaged from six grains, is $(\text{Fe}_{0.85}\text{Ca}_{0.13}\text{Mg}_{0.02})\text{SiO}_3$. Optical parameters are $2V_z = 32^\circ$ to 38° ; $n_x = 1.750$, $n_y = 1.752$, and $n_z = 1.768$. The x-ray powder pattern has 64 measured lines, with the seven strongest at (spacing, relative intensity) 3.10 (6), 2.93 (10), 2.68 (9), 2.62 (6), 2.58 (6), 2.19 (5), and 2.16 Å (6). Unit cell dimensions, based on precession and Weissenberg data, and a least squares refinement of powder data are $a = 7.55$, $b = 17.38$, $c = 6.62$, $\alpha = 82.69$, $\beta = 94.53$, $\gamma = 114.34$. These data show that it is a new mineral (phase A), a triclinic pyroxenoid-type polymorph with *Siebenerketten* analogous to pyroxmangite and synthetic "iron-rhodonite" (3).

The continuation of the clinopyroxene trend beyond the calcium minima of normal terrestrial differentiated basaltic magmas toward $\text{Ca}_{25}\text{Mg}_5\text{Fe}_{70}$ and the crystallization of phase A are indicative of unusually high silica activity (4).

Plagioclase, like clinopyroxene, shows large compositional variations over submillimeter distances. The overall range of composition is An 100 to An 60. The range detected in a fine-grained rock, 10020, is An 95 to An 67, with variation mainly from grain to grain, more calcic compositions being associated with olivine and blocky ilmenite. In a coarser rock, 10047, a similar range occurs as normal zoning in single grains. Comparison of compositions and $2V$ determinations shows correlation with high structural state curves (5).

Olivine occurs in some rocks as mainly large, early grains, commonly

Table 1. Electron microprobe analyses of some glasses from two breccias. Color of glasses in plane-polarized light: 1, yellow-brown; 2, light yellow; 3, light yellow; 4, yellow-brown; 5, colorless; 6, semiopaque.

Oxide	Sample 10065,21			Sample 10018,27		
	1*	2*	3	4	5	6
SiO ₂	38.3	42.9	43.9	38.1	40.9	41.4
TiO ₂	13.3	5.9	5.3	6.6	1.0	0.3
Al ₂ O ₃	7.0	13.8	15.5	15.0	25.5	18.9
Cr ₂ O ₃	0.4	0.3	0.2	0.2	0.1	0.15
FeO†	20.0	13.5	12.6	15.9	6.8	6.4
MnO	0.25	0.15	0.15	0.2	0.1	0.1
MgO	8.9	9.0	7.8	9.6	8.4	19.4
CaO	10.2	12.3	12.5	13.7	16.1	11.5
Na ₂ O	0.5	0.8	0.8	0.3	0.5	0.3
K ₂ O	0.05	0.05	0.1	0.01	0.01	0.01
Total	98.9	98.7	98.85	99.61	99.41	98.46

* Analyses 1 and 2 from different parts of the same glass spherule. † Total iron as FeO.

enveloped by clinopyroxene. In 10020,24 core compositions are consistently about Fo 65 and rims are zoned to about Fo 55. Comparison of these core compositions with the Fe/(Fe + Mg) ratio of the rock indicates a supercooling effect before olivine nucleated. Single crystal fragments in the breccias extend the compositional range to Fo 35.

An iron-titanium-chromium mineral (phase B) of the spinel group occurs

within or in close proximity to olivine. It is slightly birefringent, has a cell edge of 8.415 ± 0.005 Å, and a compositional formula of $\text{Fe}_{1.0}(\text{Cr}_{0.60}\text{Ti}_{0.56}\text{Fe}_{0.27}\text{Al}_{0.28}\text{Mg}_{0.19})\text{O}_4$. Most grains show marginal enrichment of iron and titanium at the expense of chromium; some have rare lamellae of ilmenite and rutile.

Tabular to lamellar ilmenite appears to have a composition close to its

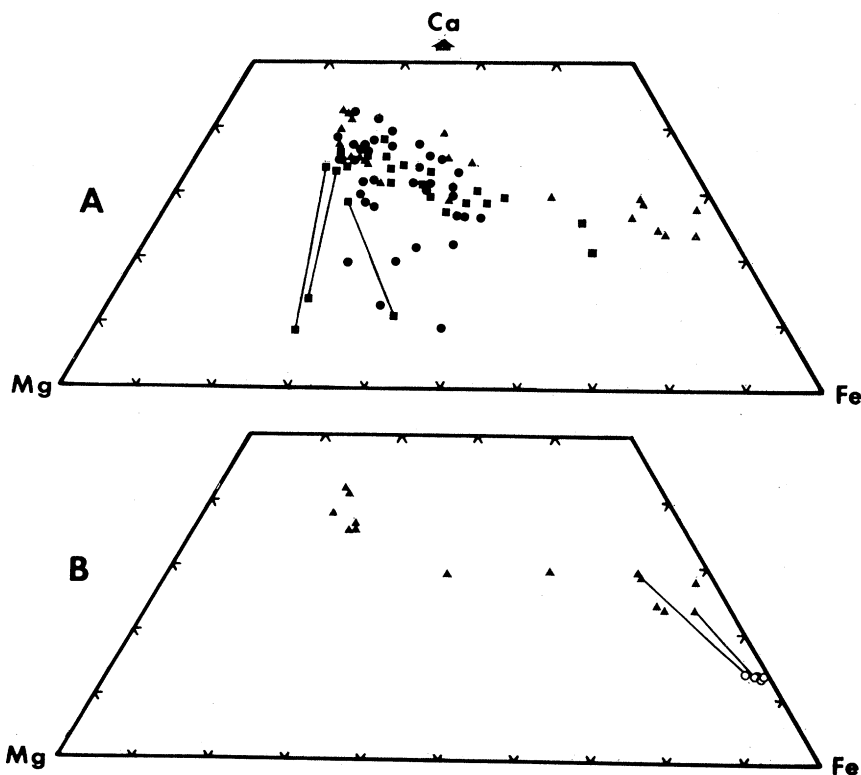


Fig. 1. (A) Plot of pyroxene compositions in terms of Ca, Mg, and Fe atomic percent for three crystalline rocks: 10017 (■), 10047 (▲), and 10069 (●). Tie lines join domains of different compositions coexisting within a single grain. (B) Plot of compositions in terms of Ca, Mg, and Fe atomic percent for one traverse across a single grain in rock 10047, and of the coexisting pyroxenoid, phase A (○). The core has an average composition $\text{Ca}_{38}\text{Mg}_{43}\text{Fe}_{19}$ and the rim $\text{Ca}_{25}\text{Mg}_5\text{Fe}_{70}$. Tie lines join phase A adjacent to the clinopyroxene.

ideal formula but slightly enriched in titanium. This suggests that the element is partly in the trivalent state (6), which would imply a very low oxygen fugacity in the magma. Some crystals show twinning, and some contain fine lamellae of rutile and a Cr-bearing mineral, possibly phase B. The x-ray powder pattern of the ilmenite is normal with no extra lines. Unit cell parameters are $a_0 = 5.088 \pm 0.005 \text{ \AA}$ and $c_0 = 14.055 \pm 0.005 \text{ \AA}$.

Minor opaque phases are troilite containing traces of Ni, Ti, and Cr, and associated blebs of native iron with trace Ni.

Low cristobalite occurs in both fine- and coarse-grained rocks, including those containing olivine. Although optically clear grains contain minor amounts of Ca, Al, Ti, and Fe (K and Mg were not detected), the x-ray powder pattern ($a_0 = 4.970 \pm 0.005 \text{ \AA}$, $c_0 = 6.931 \pm 0.005 \text{ \AA}$) is in close agreement with that of the NBS standard (7). Crystallizing with the cristobalite are potassium-barium feldspars; apatite; at least two zirconium-bearing phases, one of which is an iron-titanium-zirconium silicate (phase C) occurring as minute red-brown flakes; and in some cases a largely isotropic mesostasis rich in potash and silica. Observed in the breccias are orthopyroxene close to En 70; single grains of pigeonite; and a few meteorite fragments of nickel-iron containing up to 17 percent Ni.

The breccias and fines are in addition the source of strongly deformed crystals, glasses, and recrystallized fragments which we interpret as the products of shock metamorphism. Tensional fractures, a common feature of the larger fragments in the breccias and, to a lesser extent, of the crystalline rocks, are taken to be the result of weaker shock stresses.

However, other styles of deformation occur which we do not consider to be shock induced; in some cases stresses accompanied crystal emplacement and growth, whereas in a few fragments postcrystallization strain may have been imposed at tectonic rates. The deformation attributed to crystallization stress is most clearly seen in pyroxenes in some coarser rocks. It is commonly developed as an undulous extinction ranging over as much as 30° . In many grains the boundaries between areas of differing extinction position are sharp and coincide with color and compositional domain boundaries. In others variation in extinction position, color,

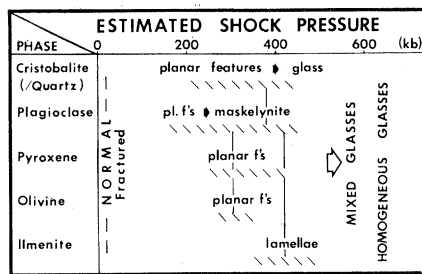


Fig. 2. A generalized scheme of shock metamorphism for the main minerals in breccia samples with estimated shock pressures. Observations have been made on normal and fractured phases, on mixed and homogeneous glasses, and in the regions indicated by diagonal patterns. Vertical lines link phases in polycrystalline fragments.

and composition takes place over a zone 10 to $25 \mu\text{m}$ wide. This zone may also be the site of narrow (1 to $3 \mu\text{m}$), curved or wavy, closely spaced features, possibly fine kinks, which differ slightly in refractive index from the host crystal. The close correlation of these features with compositional variation in the pyroxenes suggests that they result from strains induced during crystallization. This conclusion gains support from the absence of comparable deformation in coexisting plagioclase and cristobalite which are more sensitive to postcrystallization stresses.

The distinct shock deformation features seen in single and multiple mineral fragments in the breccias and fines have been assigned to a scheme of progressive shock metamorphism (Fig. 2) on the basis of the degree of development of planar features and changes in refractive index and birefringence.

Most common among the shocked minerals are clinopyroxene fragments averaging $50 \mu\text{m}$ across with nearly normal optics but containing one or two sets of planar features. The latter are up to $2 \mu\text{m}$ wide and $10 \mu\text{m}$ apart, have distinctly lower refractive indices than their host, and lie close to the zone $[\bar{h}11]$ ($h = 1, 2, 3$).

Plagioclase exhibits a comparable development of one to four sets of planar features. In most cases this development is accompanied by variable extinction and decrease in refractive index and birefringence toward the isotropic state, maskelynite. Silica phases, originally either cristobalite or possibly quartz, also contain multiple sets of planar features; large single grains with as many as eight sets of planar features have been measured. Such grains show variations in mean refractive index and

birefringence, some domains being isotropic, and others have an apparent $2V_z$ about 35° . These grains coexist with completely isotropic maskelynite.

Also coexisting with maskelynite are more strongly deformed clinopyroxenes with as many as four planar sets and a fine, mosaic undulous extinction. Similar deformation states are seen in olivine, orthopyroxene, and pigeonite. Ilmenite at this stage is not noticeably deformed, though commonly fractured and twinned. A few grains enclosed in glass are strongly disrupted and show fine striations between twin lamellae.

The glasses are considered the products of intense shock metamorphism (Fig. 2). They commonly contain schlieren of variable refractive index and show great variation in shape, composition (Table 1), vesicularity, degree of recrystallization, and character of inclusions. Some compositions (analyses 1 to 4) are comparable with the reported analyses (1); others (analyses 5 and 6) are significantly different and may be derived from biminerale assemblages.

We have not recognized tectosilicates with well-developed weak shock features as are common in large ($>1 \text{ km}$) impact craters (8); the shocked phases observed are probably the products of the small craters in the immediate vicinity of Tranquillity Base (9).

On the other hand, fragments of strongly crushed plagioclase-orthopyroxene rocks and orthopyroxene with broad kink bands resemble tectonites rather than shocked rocks, suggesting that either tectonic or crater-related faulting has occurred.

The presence of possible tectonites and the indications from the biminerale rocks and the more homogeneous mineral fragments of crystal fractionation and slow cooling at depth, point to the operation of internal lunar processes. However, the clearest evidence for an active moon comes from the fine-grained crystalline rocks. Their overall textural homogeneity and freedom from xenoliths is in strong contrast to impactites of similar grain size (10). We therefore favor generation of magma by anorogenic volcanism from a common titanium-rich source rather than by impact melting.

The crystallization and the absence of distinct phenocrysts indicate a simple magmatic history. Cooling conditions were generally rapid and characterized by supercooling, high silica activity and low fO_2 , fS_2 , and fH_2O . The unusual

mineral assemblages and metastable phases so produced owe their preservation to the apparently anhydrous environment.

J. A. V. DOUGLAS

Geological Survey of Canada,
Ottawa, Ontario

M. R. DENCE

Observatories Branch,
Department of Energy, Mines and
Resources, Ottawa, Ontario

A. G. PLANT, R. J. TRAILL
Geological Survey of Canada,
Ottawa

References and Notes

1. Lunar Sample Preliminary Examination Team, *Science* 165, 1211 (1969).
2. Crystalline rocks: 10017,23; 10020,24; 10047,25; 10069,29. Breccias: 10018,27; 10023,9; 10046,53;

- 10060,20; 10061,39; 10065,21; 10073,25. Fines: 10085,14.
 3. J. H. Whiteley and A. F. Hallimond, *J. Iron Steel Inst.* 99, 199 (1919).
 4. D. H. Lindsley and J. L. Munoz, *Amer. J. Sci.* 267A, 295 (1969).
 5. J. R. Smith, *Amer. Mineral.* 43, 1179 (1958).
 6. J. B. MacChesney and A. Muan, *ibid.* 46, 572 (1961).
 7. H. E. Swanson, M. I. Cook, E. H. Evans, J. H. deGroot, *Nat. Bur. Stds. Circ.* 539 10, 48 (1960).
 8. P. B. Robertson, M. R. Dence, M. A. Vos, *Shock Metamorphism of Natural Materials* (Mono, Baltimore, 1968), p. 433.
 9. Apollo 11 Preliminary Science Report, *NASA SP-214* (1969).
 10. M. R. Dence, *Ann. N.Y. Acad. Sci.* 123, 941 (1965); F. C. Taylor and M. R. Dence, *Canadian J. Earth Sci.* 6, 39 (1969).
 11. E. C. T. Chao, *Shock Metamorphism of Natural Materials* (Mono, Baltimore, 1968), p. 135; W. v. Engelhardt and D. Stöffler, *ibid.*, p. 159.
 12. Technical assistance of colleagues at the Geological Survey of Canada is gratefully acknowledged.
- 4 January 1970

Mineral Chemistry of Lunar Samples

Abstract. Glass spherules, glass fragments, augite, ferroaugite, titanaugite, pyroxmangite, pigeonite, hypersthene, plagioclase, potassium feldspar, maskelynite, olivine, silica, ilmenite, TiO₂, "ferropseudobrookite," spinel, ulvöspinel, native iron, nickel-iron, troilite, and chlorapatite were analyzed with the electron microprobe. There are no indications of large-scale chemical differentiation, chemical weathering, or hydrous minerals. Contributions of meteoritic material to lunar surface rocks are small. Rocks with igneous textures originated from a melt that crystallized at or near the surface, and oxygen fugacities have been low. Shock features indicate that at least some surface material is impact-produced.

Polished thin sections of loose surface fines < 1 mm in diameter (10084-97), breccias (10019-22, 10059-27, 10067-8, 10068-34), and igneous rock (10045-29) were studied by optical and electron microprobe techniques. Some of us are coinvestigators on other projects and studied breccia 10061-37 (T.E.B.) and loose surface material 10086-3 (K.K.).

Sample 10084-97 consists largely of rock fragments, feldspar, pyroxene, ilmenite, and glass spherules and glass fragments, with lesser amounts of pyroxmangite, olivine, ulvöspinel, and metallic nickel-iron. Breccias have essentially the same major phases and, in addition, accessory phases (pyroxman-

gite, pigeonite, hypersthene, maskelynite, olivine, silica, TiO₂, "ferropseudobrookite," spinel, native iron, metallic nickel-iron, troilite, chlorapatite, and silica-rich glass). Loose surface material and breccias contain a variety of rock fragments, many of which resemble in their mineralogy and chemistry the igneous rocks. However, there are also a variety of lithic fragments that are apparently not represented in the hand-specimen-sized samples. Fragments in sample 10059-27 consist largely of plagioclase [An₉₅ (95 mole percent anorthite)] and minor amounts of olivine [Fo₆₆ (66 mole percent forsterite)], augite [Fs_{15.3}En_{45.6}Wo_{39.1} (15.3 mole percent ferrosilite,

45.6 mole percent enstatite, 39.1 mole percent wollastonite)], pigeonite (Fs_{30.3}En_{61.4}Wo_{8.3}), and ilmenite (6 percent MgO by weight) resembling terrestrial anorthositic gabbros. This occurrence, in association with Ti-rich mafic rocks, is noteworthy because terrestrial anorthositic rocks also tend to be associated with Ti-rich provinces. Fragments in sample 10019-22 consist of plagioclase (An₉₅), olivine (Fo₈₁), plagioclase glass, fine-grained lath-like feldspar and pyroxene embedded in the glass, and spinel A (Table 1). One inclusion in sample 10061-37 is largely maskelynite (An₉₁), clinopyroxene (Fs_{16.3}En_{41.4}Wo_{42.3}), and orthopyroxene (Fs_{37.6}En_{58.5}Wo_{3.9}).

Sample 10045-29 is a medium-grained ophitic igneous rock containing augite, plagioclase, and ilmenite; ferroaugite, titanaugite, pigeonite, potassium feldspar, olivine, silica, native iron, troilite, and chlorapatite are present in accessory amounts.

The following is a summary of the observed phases and their compositions in the samples studied:

Calcium-rich pyroxenes contain TiO₂ (0.67 to 9.3 percent by weight) and Al₂O₃ (0.58 to 9.7 percent). All pyroxenes with more than 2 percent TiO₂ are referred to as titanaugite (1). Most grains contain Cr₂O₃ (0.1 to 0.8 percent), and the amount of Cr₂O₃ increases with increasing MgO content. Manganese monoxide ranges from 0.06 to 0.54 percent; K₂O and Na₂O rarely exceed 0.10 percent each.

Pyroxenes exhibit minor to large within-grain and grain-to-grain compositional variabilities. Major elements in larger grains vary widely across grains and even broad areas (10 to 15 μm or more) do not generally show repetitions of patterns consistent with fine-scale exsolution, although well-defined exsolution of orthopyroxene or pigeonite from augite, and augite from hypersthene have been observed in a few grains. Typical patterns across large pyroxene grains show that FeO varies

Table 1. Electron microprobe analysis of less common minerals. Compositions are given in percentages by weight.

Mineral	SiO ₂	Al ₂ O ₃	FeO	CaO	Na ₂ O	K ₂ O	Cr ₂ O ₃	TiO ₂	MnO	MgO	ZrO ₂	Total
	<i>Silicates</i>											
Potassium feldspar	64.6	19.9	0.60	0.72	0.33	13.1						99.25
Silica	96.9	1.03	0.35	0.52	0.05	0.25						99.10
	<i>Oxides</i>											
Ulvöspinel		1.88	62.2	0.03			3.5	32.7	0.22	0.04		100.57
Spinel A		68.0	3.33				2.16			25.9		99.39
Spinel B		6.0	46.3				19.3	23.0		4.3		98.9
"Ferropseudobrookite"		1.48	14.7	0.32			1.94	71.4	0.07	8.7	0.05	98.66